Reduction of Numerical Dispersion in FDTD Method Through Artificial Anisotropy

Jaakko S. Juntunen and Theodoros D. Tsiboukis, *Member, IEEE*

Abstract—In this paper, a simple and computationally low-cost modification of the standard finite-difference time-domain (FDTD) algorithm is presented to reduce numerical dispersion in the algorithm. Both two- and three-dimensional cases are considered. It is shown that the maximum error in phase velocity can be reduced by a factor of 2–7, depending on the shape of the FDTD cell. Although the reduction procedure is optimal for only single frequency, numerical examples show that the proposed method can also improve the accuracy significantly in wide-band inhomogeneous problems.

Index Terms—FDTD method, numerical dispersion.

I. INTRODUCTION

NUMERICAL dispersion is an undesired nonphysical effect inherently present in the finite-difference time-domain (FDTD) algorithm. In short, numerical dispersion means dependence of wave propagation velocity on frequency. Herein, we also include in the term the dependence of velocity on propagation direction. The latter is sometimes called numerical anisotropy. In qualitative terms, dispersion causes distortion of waveforms. Frequency dependence causes high-frequency content of a wave to lag, while direction dependence causes spherical waveforms to become slightly cubical.

There are several problems associated with numerical dispersion. First, it causes cumulative phase error. If a device is based on phase cancellation, even an apparently small error in wave propagation velocity may cumulate phase error to unacceptable amounts. Equivalently, phase error appears as mislocation of resonances in the frequency domain. Sometimes, it is possible to pre-estimate the effect of the dispersion error, and use the estimation to choose proper spatial resolution for the problem [1]. In some cases, the numerical dispersion can be eliminated in post-processing [2]. This elimination is rarely possible since it is based on the assumption that there are waves propagating in only one direction.

Another possible trouble with the numerical dispersion is nonphysical refraction [3]. If the cell shape varies over the grid, a wave experiences different numerical dispersion in different parts of the grid. This corresponds to inhomogeneous medium, and refraction takes place. In some problems, it is indeed necessary to vary the cell shape quite dramatically, e.g.,

in [4], the width-to-length ratio of a two-dimensional (2-D) cell varies a factor of 12.5.

A different FDTD algorithm is proposed in [5], which is equivalent to the so-called symmetrical-condensed-node transmission-line matrix method (SCN–TLM). The dispersion errors in SCN–TLM are less than in the standard FDTD technique [6], [7]. A distinct disadvantage of the SCN–TLM formulation though, is the need of extensive memory requirements as opposed to the standard FDTD implementation. Another possibility is to use fourth-order spatial differencing in the algorithm [8]. However, associated problems are encountered as more smoothness is assumed from the field quantities, especially on the material boundaries.

The present reduction method is based on carefully speeding up the wave propagation by introducing anisotropy parameters into the algorithm. A detailed Fourier-mode analysis is given for the determination of the optimal anisotropy parameters. Several simulation examples confirm the theory. Wide-band problems are also discussed.

II. NUMERICAL DISPERSION RELATION IN 2-D

Let us consider electrically anisotropic medium in 2-D and the TE mode. Let the relative permittivity tensor be diagonal, i.e., $\underline{\varepsilon}_r = \text{diag}(\varepsilon_x, \varepsilon_y)$. The stability condition of the FDTD algorithm for this problem is

$$\Delta t \leq \frac{1}{c_0 \sqrt{\dfrac{1}{\varepsilon_y \Delta x^2} + \dfrac{1}{\varepsilon_x \Delta y^2}}}. \tag{1}$$

Here, c_0 is the speed of light in free space. The derivation of the dispersion relation is canonical. A wave is expanded into plane waves of the form

$$\Psi = \Psi_0 e^{j(\omega t - k_x x - k_y y)} \tag{2}$$

and the FDTD update equations are applied to these waves.

The resulting numerical dispersion relation for the TE mode is

$$\left(\frac{1}{c_0 \Delta t} \sin\left(\frac{\omega \Delta t}{2} \right) \right)^2 = \frac{\sin^2\left(\dfrac{k_x \Delta x}{2} \right)}{\varepsilon_y \Delta x^2} + \frac{\sin^2\left(\dfrac{k_y \Delta y}{2} \right)}{\varepsilon_x \Delta y^2}. \tag{3}$$

The TM mode does not "see" the electric anisotropy. The dual situation can be obtained by replacing the relative permittivities by relative permeabilities.

In (3), we write the numerical wave vector as $(k_x, k_y) = (\tilde{k} \cos \alpha, \tilde{k} \sin \alpha)$, where $\tilde{k}$ is the numerical wavenumber and

α is the angle between the propagation direction and positive x-axis. The dispersion characteristics of the FDTD grid are expressed in a clear way by plotting for each frequency the velocity of a plane wave in the grid versus the angle α.

Let us now express (3) in a form that is independent of physical dimensions. For this, let us introduce a parameter that defines the shape of a single FDTD cell

$$Z = \frac{\Delta x}{\Delta y}. \tag{4}$$

Furthermore, we define a spatial resolution coefficient that relates the wavelength and cell dimensions

$$R = \frac{\lambda}{\sqrt{\Delta x^2 + \Delta y^2}} \tag{5}$$

where $\lambda = c_0/f$ is the wavelength in the vacuum (not in the numerical grid). Let us also define a Courant coefficient $q \leq 1$ in accordance with (1)

$$\Delta t = q \frac{1}{c_0 \sqrt{\dfrac{1}{\varepsilon_y \Delta x^2} + \dfrac{1}{\varepsilon_x \Delta y^2}}}. \tag{6}$$

Using (4) and (6)

$$c_0 \Delta t = q \frac{\Delta y Z \sqrt{\varepsilon_x \varepsilon_y}}{\sqrt{\varepsilon_x + \varepsilon_y Z^2}} \tag{7}$$

and using (4) and (5)

$$\lambda = R \sqrt{1 + Z^2} \Delta y. \tag{8}$$

Since $\omega = (2\pi c_0/\lambda)$, we get from (7) and (8)

$$\frac{\omega \Delta t}{2} = \pi \frac{c_0 \Delta t}{\lambda} = \frac{\pi q Z \sqrt{\varepsilon_x \varepsilon_y}}{R\sqrt{1 + Z^2}\sqrt{\varepsilon_x + \varepsilon_y Z^2}}. \tag{9}$$

Let us denote by $\tilde{\lambda}$ the wavelength in the grid and write $\tilde{k} = (2\pi/\tilde{\lambda})$. Using (8), we have $\tilde{k}\Delta y = (2\pi/R\sqrt{1+Z^2})(\lambda/\tilde{\lambda})$. The interesting quantity is the relative numerical velocity $A := (c^*/c_0) = (\tilde{\lambda}/\lambda)$, where c^* is the propagation velocity in the grid. Therefore, we finally write

$$\frac{\tilde{k}\Delta y}{2} = \frac{1}{A}\frac{\pi}{R\sqrt{1+Z^2}}. \tag{10}$$

Substituting (4)–(10) into (3) yields the dimensionless numerical dispersion relation

$$\frac{\varepsilon_x + \varepsilon_y Z^2}{\varepsilon_x \varepsilon_y q^2 Z^2} \sin^2\left(\frac{\pi q Z \sqrt{\varepsilon_x \varepsilon_y}}{R\sqrt{1+Z^2}\sqrt{\varepsilon_x + \varepsilon_y Z^2}}\right)$$
$$= \frac{\sin^2\left(\dfrac{\pi \sin\alpha}{AR\sqrt{1+Z^2}}\right)}{\varepsilon_x} + \frac{\sin^2\left(\dfrac{\pi Z \cos\alpha}{AR\sqrt{1+Z^2}}\right)}{\varepsilon_y Z^2}. \tag{11}$$
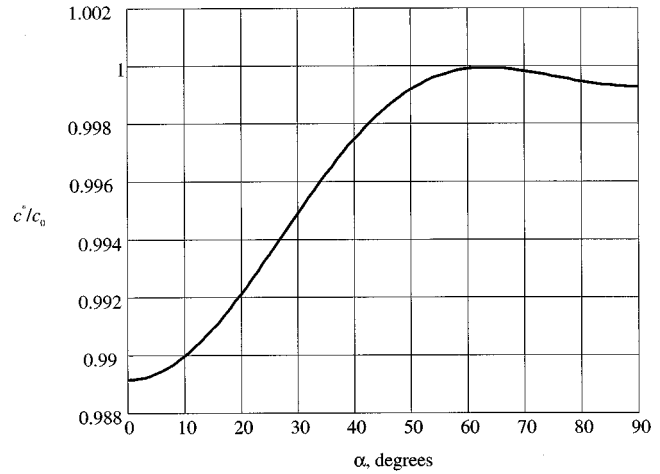

Fig. 1. Relative numerical velocity. $Z = 2$, $R = 10$, $q = 0.99$.
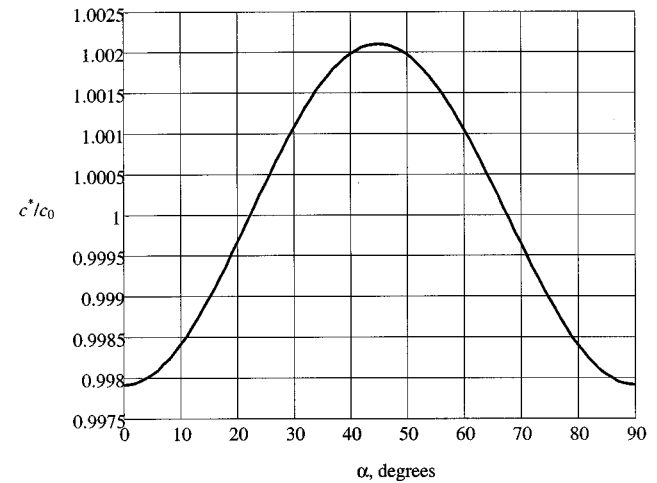

Fig. 2. Relative numerical velocity after correction. $Z = 2$, $R = 10$, $q = 0.99$, $\varepsilon_x = 1.002\,717$, $\varepsilon_y = 0.982\,972$.

The numerical solution of (11) for A is rather straightforward for a given set of parameters Z, q, R, ε_x, ε_y, and α.

III. DISPERSION REDUCTION IN 2-D THROUGH ε_x AND ε_y

Our purpose is to find parameters ε_x and ε_y such that A will be close to one for all propagation directions. Fig. 1 illustrates the solution $A(\alpha)$ from (11) for a typical case with $\varepsilon_x = \varepsilon_y = 1$, $Z = 2$, $R = 10$, and $q = 0.99$. Fig. 2 illustrates the solution of (11) for the same case, except anisotropy parameters $\varepsilon_x = 1.002\,717$ and $\varepsilon_y = 0.982\,972$ are used. The maximum dispersion error is reduced from 1.1% to 0.22%.

In [8, Sec. 5.7], a kind of optimization is presented for a square cell. There, a correction coefficient is introduced to compensate the effect of choosing $q < 1$, whereas the more dominant effect of the cell shape is not discussed.

To find the correction parameter values, we start by determining the values of ε_x and ε_y that yield $A = 1$ along the coordinate directions $\alpha = 0°$ and $\alpha = 90°$. Setting $A = 1$,
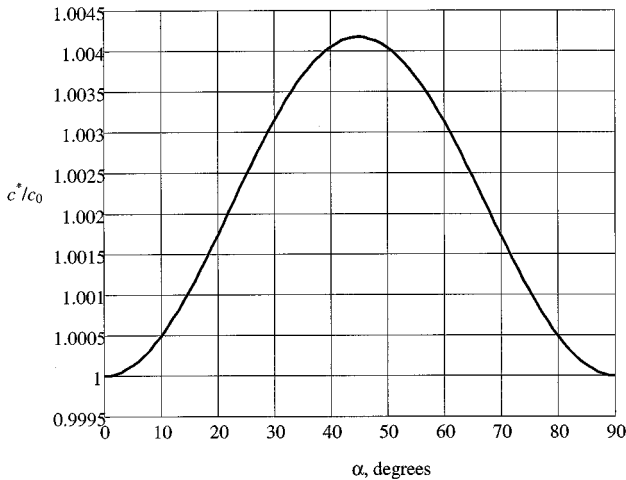
Fig. 3. Relative numerical velocity after partial correction. $Z = 2$, $R = 10$, $q = 0.99$, $\varepsilon_x = 0.998551$, $\varepsilon_y = 0.978969$.

$\alpha = 90°$ and solving for ε_x in the right-hand side (RHS) of (11) gives

$$\varepsilon_x = \frac{\varepsilon_x \varepsilon_y q^2 Z^2}{\varepsilon_x + \varepsilon_y Z^2} \frac{\sin^2\left(\dfrac{\pi}{R\sqrt{1+Z^2}}\right)}{\sin^2\left(\dfrac{\pi q Z \sqrt{\varepsilon_x \varepsilon_y}}{R\sqrt{1+Z^2}\sqrt{\varepsilon_x + \varepsilon_y Z^2}}\right)}. \quad (12)$$

Similarly, setting $A = 1$, $\alpha = 0°$ and solving now for ε_y gives

$$\varepsilon_y = \frac{\varepsilon_x \varepsilon_y q^2}{\varepsilon_x + \varepsilon_y Z^2} \frac{\sin^2\left(\dfrac{\pi Z}{R\sqrt{1+Z^2}}\right)}{\sin^2\left(\dfrac{\pi q Z \sqrt{\varepsilon_x \varepsilon_y}}{R\sqrt{1+Z^2}\sqrt{\varepsilon_x + \varepsilon_y Z^2}}\right)}. \quad (13)$$

Dividing (12) by (13) leads to

$$\frac{\varepsilon_x}{\varepsilon_y} = Z^2 \frac{\sin^2\left(\dfrac{\pi}{R\sqrt{1+Z^2}}\right)}{\sin^2\left(\dfrac{\pi Z}{R\sqrt{1+Z^2}}\right)}. \quad (14)$$

Solving (14) for ε_x, then inserting the result into (12), and solving for ε_y yields

$$a := \sin\left(\frac{\pi}{R\sqrt{1+Z^2}}\right)$$
$$b := \sin\left(\frac{\pi Z}{R\sqrt{1+Z^2}}\right)$$
$$\varepsilon_y = \frac{R^2(1+Z^2)}{\pi^2 q^2 Z^2}\left(1+\frac{b^2}{a^2}\right)\arcsin\left(\frac{qab}{\sqrt{a^2+b^2}}\right)^2. \quad (15)$$

ε_x can then be easily found from (14). For the model problem ($Z = 2$, $R = 10$, $q = 0.99$), we obtain $\varepsilon_x = 0.998551$ and $\varepsilon_y = 0.978969$. Fig. 3 illustrates the corresponding $A(\alpha)$.

We see that the curve in Fig. 3 is symmetric and has a maximum at $\alpha = 45°$. This is not a coincidence, but true in general. The strategy is to determine the maximum deviation of A from
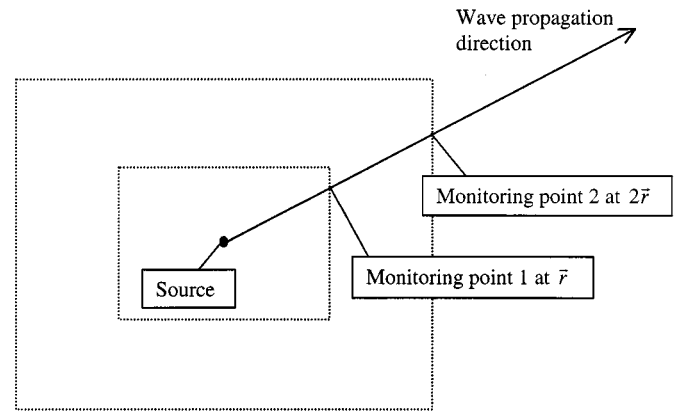

Fig. 4. Monitoring surfaces for measuring the wave propagation velocity in a simulation.

unity at this stage (about 0.0042 in Fig. 3) and to redefine ε_x and ε_y to slow down the wave velocity by half of that maximum.

The key to the last step is that the maximum of $A(\alpha)$ (after tuning ideal propagation along coordinate directions) *does not depend much on Z and not at all on q*. This appears to be due to the "lucky" choice of R in units of diagonal length of the cell. Thus, we find a good approximation of the maximum of A by choosing $q = Z = 1$ in (11), (14), and (15). Setting then $\alpha = 45°$ in (11) gives

$$A_{\max} = \frac{\pi}{2R \arcsin\left(\dfrac{\sin(\pi/R\sqrt{2})}{\sqrt{2}}\right)}. \quad (16)$$

Thus, the maximum deviation of A from unity is now $Q := (A_{\max} - 1)$. Setting $A = 1 - (Q/2)$ along axial directions, as in (12)–(15), yields the optimal parameter values ε_x and ε_y. A short Matlab-code cmp2D.m is found in the Appendix for determination of the optimal parameters. We will refer to a simulation with the correction parameters as the "corrected FDTD."

IV. VERIFICATION OF THE CORRECTION IN 2-D

To verify the predictions of the previous sections, a single H_z-component is excited in the middle of a TE structure. To measure the wave propagation velocity in the simulation, two rectangular "monitoring surfaces" are defined, as shown in Fig. 4. The program looks for the time instants during which the nth maximum of the incident wave reaches an inner monitoring point at $\vec{r}$ and the corresponding outer monitoring point at $2\vec{r}$. Knowing the traveled distance and time, velocity can be calculated.

Fig. 5 illustrates the effect of the correction in an actual simulation. A thin cell and coarse resolution is used here ($Z = 5$, $R = 5$, $q = 0.99$), and a reduction of maximum dispersion error from over 7% to less than 1% is obtained. This represents a case that is close to the practical limits of the standard FDTD method in terms of cell shape and resolution.

V. NUMERICAL DISPERSION RELATION IN 3-D

In this section, the full three–dimensional (3-D) problem is discussed. Let us consider a material that is both magnetically
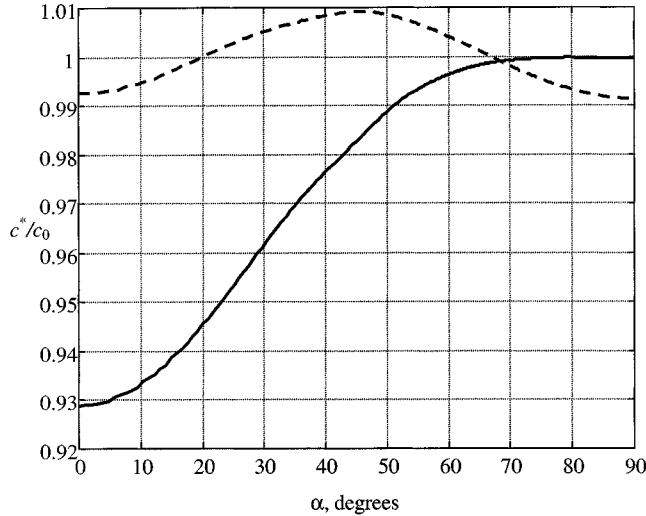
Fig. 5. Relative numerical velocity curves from simulations: standard FDTD (solid line) and corrected FDTD (dashed line). $Z = 5$, $R = 5$, $q = 0.99$.

and electrically anisotropic: $\underline{\underline{\varepsilon}}_r = \text{diag}(\varepsilon_x, \varepsilon_y, \varepsilon_z)$, $\underline{\underline{\mu}}_r = \text{diag}(\mu_x, \mu_y, \mu_z)$. Recall that a Fourier mode

$$\Psi = \Psi_0 e^{j(\omega t - k_x x - k_y y - k_z z)} \qquad (17)$$

is an eigenfunction of the finite-differential operators used in the FDTD

$$D_t \Psi = j \frac{2}{\Delta t} \sin\left(\frac{\omega \Delta t}{2}\right) \Psi =: j K_t \Psi$$

$$D_s \Psi = -j \frac{2}{\Delta s} \sin\left(k_s \frac{\Delta s}{2}\right) \Psi =: j K_s \Psi \qquad (18)$$

where s stands for x, y, or z. Using (18), we can write the numerical Maxwell's equations into form

$$\mu_0 K_t \underline{\underline{\mu}} \vec{H} = \underline{\underline{K}} \vec{E} \qquad (19)$$

$$\varepsilon_0 K_t \underline{\underline{\varepsilon}} \vec{E} = -\underline{\underline{K}} \vec{H} \qquad (20)$$

where

$$\underline{\underline{K}} = \begin{bmatrix} 0 & K_z & -K_y \\ -K_z & 0 & K_x \\ K_y & -K_x & 0 \end{bmatrix}. \qquad (21)$$

Combining (19) and (20), $\vec{E}$ must satisfy an eigenvalue problem

$$\underline{\underline{\varepsilon}}^{-1} \underline{\underline{K}} \underline{\underline{\mu}}^{-1} \underline{\underline{K}} \vec{E} = -\frac{K_t^2}{c_0^2} \vec{E}. \qquad (22)$$

In general, $\underline{\underline{\varepsilon}}^{-1} \underline{\underline{K}} \underline{\underline{\mu}}^{-1} \underline{\underline{K}}$ has two different nonzero eigenvalues. However, if $\underline{\underline{\mu}} = \underline{\underline{\varepsilon}}$, (22) has a double eigenvalue $-(\varepsilon_y^{-1} \varepsilon_z^{-1} K_x^2 + \varepsilon_x^{-1} \varepsilon_z^{-1} K_y^2 + \varepsilon_x^{-1} \varepsilon_y^{-1} K_z^2)$, and the dispersion relation reads

$$\frac{K_t^2}{c_0^2} = \frac{K_x^2}{\varepsilon_y \varepsilon_z} + \frac{K_y^2}{\varepsilon_x \varepsilon_z} + \frac{K_z^2}{\varepsilon_x \varepsilon_y} \qquad (23)$$

or

$$\left(\frac{1}{c_0 \Delta t} \sin\left(\frac{\omega \Delta t}{2}\right)\right)^2 = \frac{\sin^2\left(\frac{k_x \Delta x}{2}\right)}{\varepsilon_y \varepsilon_z \Delta x^2} + \frac{\sin^2\left(\frac{k_y \Delta y}{2}\right)}{\varepsilon_x \varepsilon_z \Delta y^2}$$
$$+ \frac{\sin^2\left(\frac{k_z \Delta z}{2}\right)}{\varepsilon_x \varepsilon_y \Delta z^2}. \qquad (24)$$

The corresponding stability criterion is

$$\Delta t \leq \frac{1}{c_0 \sqrt{\dfrac{1}{\varepsilon_y \varepsilon_z \Delta x^2} + \dfrac{1}{\varepsilon_x \varepsilon_z \Delta y^2} + \dfrac{1}{\varepsilon_x \varepsilon_y \Delta z^2}}}. \qquad (25)$$

Let us again define dimensionless parameters

$$Z_y = \frac{\Delta x}{\Delta y}, \ Z_z = \frac{\Delta x}{\Delta z}, \ R = \frac{\lambda}{\sqrt{\Delta x^2 + \Delta y^2 + \Delta z^2}} \qquad (26)$$

and a Courant coefficient $q \leq 1$ such that (25) holds. After a little algebra, as in Section II, we end up with a dimensionless dispersion relation

$$\frac{\varepsilon_x + \varepsilon_y Z_y^2 + \varepsilon_z Z_z^2}{q^2 \varepsilon_x \varepsilon_y \varepsilon_z}$$
$$\cdot \sin^2\left(\frac{\pi q \sqrt{\varepsilon_x \varepsilon_y \varepsilon_z}}{R \sqrt{1 + Z_y^{-2} + Z_z^{-2}} \sqrt{\varepsilon_x + \varepsilon_y Z_y^2 + \varepsilon_z Z_z^2}}\right)$$
$$= \frac{1}{\varepsilon_y \varepsilon_z} \sin^2\left(\frac{\pi \sin\theta \cos\varphi}{AR\sqrt{1 + Z_y^{-2} + Z_z^{-2}}}\right)$$
$$+ \frac{Z_y^2}{\varepsilon_x \varepsilon_z} \sin^2\left(\frac{\pi \sin\theta \sin\varphi}{ARZ_y\sqrt{1 + Z_y^{-2} + Z_z^{-2}}}\right)$$
$$+ \frac{Z_z^2}{\varepsilon_x \varepsilon_y} \sin^2\left(\frac{\pi \cos\theta}{ARZ_z\sqrt{1 + Z_y^{-2} + Z_z^{-2}}}\right) \qquad (27)$$

where θ and φ are the polar and azimuth angles, respectively, of the wave propagation direction, and A is again the ratio of numerical to ideal velocity in that direction.

VI. DISPERSION REDUCTION IN 3-D THROUGH ε_x, ε_y, AND ε_z

The procedure for finding the proper correction parameters is similar to that in Section III. A short Matlab-code cmp3D.m is found in the Appendix for that purpose. One has to remember to *use the same parameters in the permeability tensor also*. For "needle"-type cells (Z_y and Z_z both large), the solution of (27) with and without correction predicts that the maximum dispersion error will be reduced by a factor of about seven. However, typical values for the reduction factor are 2–5.

VII. VERIFICATION OF THE CORRECTION IN 3-D

To verify the predicted correction, a single H_z-component is excited in the origin to represent a point magnetic dipole source. In Fig. 6, the phase velocities from actual simulations
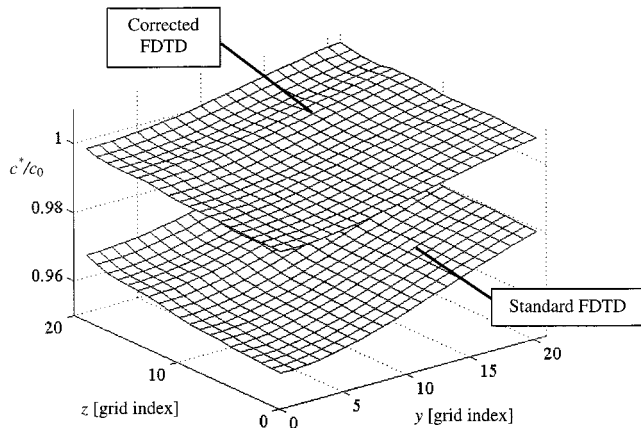
Fig. 6. Comparison of corrected and uncorrected simulated phase velocity to the ideal physical phase velocity. Problem $Z_y = 1.5$, $Z_z = 3$, $R = 5$ and monitoring surfaces parallel to yz-plane are considered.

Fig. 7. Inhomogeneous infinite waveguide structure modeled in example 1.

are compared, with and without correction. The monitoring surfaces are parallel to the yz-plane. Clearly, the dispersion error is again reduced significantly. A coarse resolution $R = 5$ and a "brick"-type cell shape $\Delta x : \Delta y : \Delta z = 3 : 2 : 1$ are used. For propagation along other directions than indicated in Fig. 6, the corrected dispersion error remains within $\pm 1\%$, while the dispersion error without correction reaches -4%.

VIII. WIDE-BAND PROBLEMS

Since one of the key advantages of the FDTD method is the possibility to perform wide-band simulations, it is clearly a disadvantage of the proposed correction method that it is optimal for only one frequency. However, due to other advantages, FDTD is sometimes used in single-frequency problems, e.g., [4].

Fortunately, investigating the dispersion relation (27) with fixed correction parameters and varying resolution R, one finds that the dispersion reduction is almost optimal in a reasonable band around the value R_0 used for designing the correction parameters. The following descriptive conclusions can be made.

- For frequencies higher than f_0 (= design frequency for the correction parameters) the maximum dispersion error is always less than in standard FDTD.
- With very low frequencies, the reduction is not of much use since the dispersion is very small anyway.

Experiments suggest using correction parameters, which correspond to the *lowest* frequency of the band, not the central frequency. If the band starts from dc, one could consider standard FDTD for the lowest subband and corrected FDTD for the higher subbands. This implies two separate simulations for the same problem, but these are totally independent and can be performed simultaneously using two processors. With one processor though, double simulation time is needed, but the overall saving can still be high. In Section IX, two wide-band problems are discussed. Quite often, we are interested in only relative narrow frequency bands where the reduction scheme can be used alone.
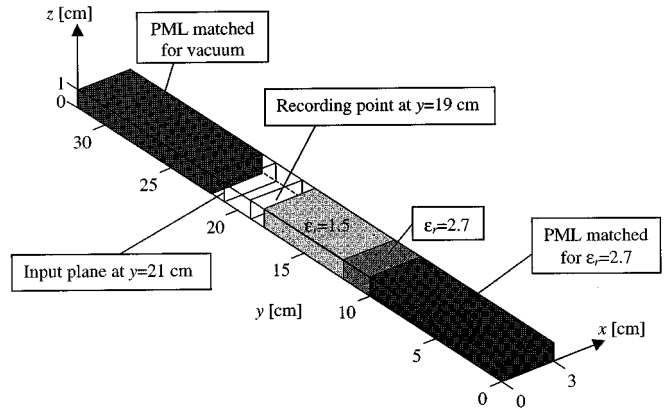
IX. SIMULATION TESTS WITH INHOMOGENEOUS PROBLEMS

If there are only different isotropic dielectrics and perfect conductors present, the proposed correction can be easily extended to an inhomogeneous problem. A different set of anisotropy parameters is designed for each dielectric. In the material interfaces, all parameter values are averaged, as proposed in [9].

Here, we consider two inhomogeneous wide-band examples. The first example is a 3-D waveguide filled with three dielectrics: dielectric-1 (vacuum) for $y = 18\,\text{cm} \cdots + \infty$, dielectric-2 ($\varepsilon_r = 1.5$) for $y = 12, \cdots, 18$ cm and dielectric-3 ($\varepsilon_r = 2.7$) for $y = -\infty, \cdots, 12$ cm (Fig. 7). The dimensions of the cross section of the waveguide are $a = 3$ cm and $b = 1$ cm. To model the infinite ends, generalized 20-layer perfectly matched layer (PML) absorbing boundary conditions are used, especially suitable for anisotropic problems [10]. The cell dimensions used are $\Delta x = 0.3$ cm, $\Delta y = 0.5$ cm, and $\Delta z = 0.2$ cm. The y-direction is along the waveguide axis.

A modulated Gaussian pulse in TE_{10} mode is launched at the input plane at $y = 21$ cm. The pulse contains approximately the frequency range from 5.2 to 7.5 GHz. The excitation is separated from the field interactions [11]. The E_z-component of the wave is recorded in the middle of the cross section of the waveguide at $y = 19$ cm. The anisotropy parameters are optimized to frequency $f_{\text{fix}} = 5.2\,\text{GHz}$ ($R = 9.3526$ in the vacuum, $R = 7.6363$ in the dielectric-2, and $R = 5.6918$ in the dielectric-3) as follows:

$$\varepsilon_x = 0.993\,372 \quad \varepsilon_y = 1.009\,350 \quad \varepsilon_z = 0.988\,441$$
$$\text{for vacuum}$$
$$\varepsilon_x = 0.989\,436 \quad \varepsilon_y = 1.013\,498 \quad \varepsilon_z = 0.982\,057$$
$$\text{for dielectric-2}$$
$$\varepsilon_x = 0.979\,945 \quad \varepsilon_y = 1.023\,675 \quad \varepsilon_z = 0.966\,741$$
$$\text{for dielectric-3}.$$

$q = 0.99$ in all calculations. In the dielectrics, the Courant coefficient q_d is not known *a priori* (since only q in vacuum is chosen), but is needed in the evaluation of the anisotropy parameters. For that purpose, a good enough approximation of q_d is $q/\sqrt{\varepsilon_r}$.
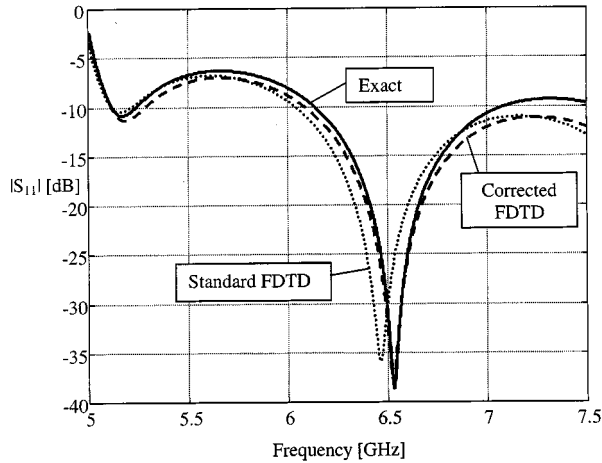
Fig. 8. $|S_{11}|$ parameter of the structure in Fig. 7. The dispersion reduction parameters are optimized for $f = 5.2$ GHz. Standard FDTD ($\cdots\cdots$), corrected FDTD (- - - -), and exact solution (—).
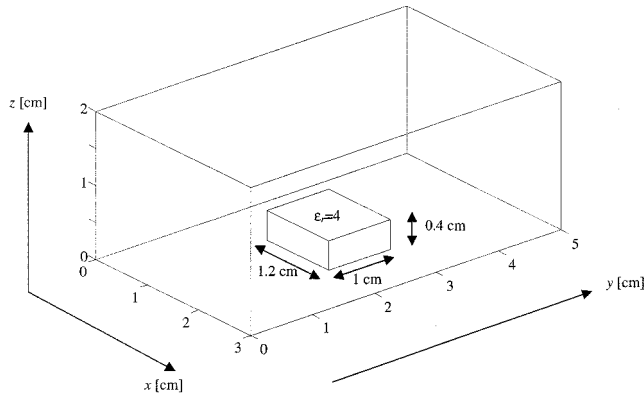

Fig. 9. Inhomogeneous cavity modeled in example 2.

The $|S_{11}|$ parameter is computed. The exact solution is

$$|S_{11}| = \left| \frac{\rho_{12} + \rho_{23}e^{-2\gamma_2 L}}{1 + \rho_{12}\rho_{23}e^{-2\gamma_2 L}} \right|. \tag{28}$$

Here, γ_2 is the propagation constant of the waveguide filled with the dielectric-2, L is the thickness of the dielectric-2 (6 cm), and $\rho_{ij} = (\eta_j - \eta_i)/(\eta_j + \eta_i)$, where (η_k) is the characterisitc impedance of the TE_{10} mode of the waveguide filled with the dielectric-k.

Fig. 8 presents the results. Standard FDTD mislocates the main resonance peak -68 MHz and $+2.7$ dB. Using the correction, the peak is mislocated only -4 MHz and $+0.7$ dB. The conclusion is that, especially around the main resonance, the correction improves the results significantly, even more than expected. A qualitative explanation for that is that, for the corrected FDTD, the dispersion error is well balanced, i.e., the waves will propagate a bit too slowly toward some directions and a bit too fast toward some others, and an advantageous averaging takes place.

The second example is an inhomogeneous cavity shown in Fig. 9. The dielectric piece ($\varepsilon_r = 4.0$) represents a tuning element of the cavity resonator. The lowest TE_{101} resonance of the cavity without the dielectric piece occurs at 5.827 GHz. The reference resonance frequency for the cavity with the dielectric is found using a standard FDTD and a dense mesh having $40 \times 40 \times 40$ cells, corresponding resolutions $R = 33.4$ in the vacuum and $R = 16.7$ in the dielectric. The cavity is excited by a point source having a Gaussian time variation, and the E_z-component is recorded. The reference resonance is found to be 5.584 GHz. For the comparisons, we use standard FDTD in $10 \times 10 \times 10$ and $20 \times 20 \times 20$ meshes, and corrected FDTD in a $10 \times 10 \times 10$ mesh. The reduction is optimized to 5.0 GHz ($R = 9.7267$ in the vacuum and $R = 4.8633$ in the dielectric), giving the following compensation parameter values:

$$\varepsilon_x = 0.993\,874 \quad \varepsilon_y = 1.008\,637 \quad \varepsilon_z = 0.989\,314$$
$$\text{for vacuum}$$
$$\varepsilon_x = 0.971\,911 \quad \varepsilon_y = 1.032\,297 \quad \varepsilon_z = 0.953\,918$$
$$\text{for dielectric.}$$

The standard FDTD with a $10 \times 10 \times 10$ mesh gives 5.557 GHz (-27 MHz compared to the reference solution), while the corrected FDTD gives 5.580 GHz (-4 MHz). The standard FDTD with a $20 \times 20 \times 20$ mesh gives 5.578 GHz (-6 MHz). Hence, corrected FDTD in a coarse mesh gives about the same result than standard FDTD in a dense mesh having eight times more cells and using 16 times more central processing unit (CPU) time.

X. CONCLUSIONS

This paper introduces a simple correction procedure for reduction of the numerical dispersion in the FDTD algorithm. Compared to the standard algorithm, the method does not introduce any additional computational cost and requires only a modest amount of reprogramming. However, the method can be of high value in problems where the numerical dispersion is expected to play a major role. It is demonstrated through several examples that even though the correction is optimal only for a single frequency, the method can still yield significantly improved performance in wide-band inhomogeneous problems.

APPENDIX

Matlab-code cmp2D.m evaluates the optimal anisotropy parameters ε_x and ε_y for a 2-D problem, for given resolution R, cell shape Z, and Courant-coefficient q

```
function [ex, ey]=cmp2D(R, Z, q);
% Jaakko Juntunen 20.9.1999.
Amax =
  pi/(2*R*asin(sin(pi/(R*sqrt(2)))/sqrt(2)));
Q = Amax - 1;
a = sin(pi/((1 - Q/2)*R*sqrt(1 + Z^2)));
b = sin(pi*Z/((1 - Q/2)*R*sqrt(1 + Z^2)));
ey = R^2*(1 + Z^2)/(pi*q*Z)^2*(1 +
  b^2/a^2)*asin(q*a*b/sqrt(a^2 + b^2))^2;
ex = Z^2*a^2/b^2*ey;
```

Matlab-code cmp3D.m evaluates the optimal anisotropy parameters ε_x, ε_y and ε_z for a 3-D problem, for given resolution R, cell shape parameters Z_y and Z_z, and Courant-coefficient q

```
function [ex, ey, ez]=cmp3D (R, Zy, Zz, q);
% Jaakko Juntunen 20.9.1999.
Amax =
  pi/(3*R*asin(sin(pi/(R*sqrt(3)))/sqrt(3)));
Q = Amax - 1;
K1 = pi/(R*sqrt(1 + 1/Zy^2 + 1/Zz^2));
a = sin(K1/(1 - Q/2))^2/(Zy^2*sin(K1/((1 -
  Q/2)*Zy))^2);
b = sin(K1/(1 - Q/2))^2/(Zz^2*sin(K1/((1 -
  Q/2)*Zz))^2);
K2 = sqrt(1 + a*Zy^2 + b*Zz^2);
ex = K2/(K1*q*sqrt(a*b))*asin(q*sin(K1/(1 -
  Q/2))/K2);
ey = a*ex;
ez = b*ex;
```

REFERENCES

[1] A. C. Cangellaris, "Numerical stability and numerical dispersion of a compact 2-D/FDTD method used for the dispersion analysis of waveguides," *IEEE Microwave Guided Wave Lett.*, vol. 3, pp. 3–5, Jan. 1993.

[2] J. G. Maloney, K. L. Schlager, and G. S. Smith, "A simple FDTD model for transient excitation of antennas by transmission lines," *IEEE Trans. Antennas Propagat.*, vol. 42, pp. 289–292, Feb. 1994.

[3] A. Taflove and K. R. Umashankar, "The finite-difference time-domain method for numerical modeling of electromagnetic wave interactions," *Electromag.*, vol. 10, no. 1-2, pp. 105–126, 1990.

[4] J. Ala-Laurinaho, T. Hirvonen, J. Tuovinen, and A. V. Räisänen, "Numerical modeling of a nonuniform grating with FDTD," *Microwave Opt. Technol. Lett.*, vol. 15, pp. 134–139, June 1997.

[5] Z. Chen, M. M. Ney, and W. J. R. Hoefer, "A new finite-difference time-domain formulation and its equivalence with the TLM symmetrical condensed node," *IEEE Trans. Microwave Theory Tech.*, vol. 39, pp. 2160–2169, Dec. 1991.

[6] L. De Menezes, C. Eswarappa, and W. J. R. Hoefer, "A comparative study of dispersion errors and performance of absorbing boundary conditions in SCN–TLM and FDTD," *13th Annu. Rev. Progress Appl. Comput. Electromag. Dig.*, pp. 673–678, March 17–21, 1997.

[7] M. Krumpholz and P. Russer, "On the dispersion in TLM and FDTD," *IEEE Trans. Microwave Theory Tech.*, vol. 42, pp. 1275–1279, July 1994.

[8] A. Taflove, *Computational Electrodynamics—The Finite-Difference Time-Domain Method*. Norwood, MA: Artech House, 1995.

[9] X. Zhang and K. K. Mei, "Time-domain finite difference approach to the calculation of the frequency-dependent characteristics of microstrip discontinuities," *IEEE Trans. Microwave Theory Tech.*, vol. 36, pp. 1775–1787, Dec. 1988.

[10] A. P. Zhao, J. Juntunen, and A. V. Räisänen, "Generalized material independent PML absorbers for the FDTD simulation of electromagnetic waves in arbitrary anisotropic dielectric and magnetic media," *IEEE Microwave Guided Wave Lett.*, vol. 8, pp. 52–54, Feb. 1998.

[11] A. P. Zhao, A. V. Räisänen, and S. R. Cvetkovic, "A fast and efficient FDTD algorithm for the analysis of planar microstrip discontinuities by using a simple source excitation scheme," *IEEE Microwave Guided Wave Lett.*, vol. 5, pp. 341–323, Oct. 1995.

Jaakko S. Juntunen was born in Tornio, Finland, in 1971. He received the Master of Science degree (with distinction) in technical mathematics and the Licentiate of Technology degree from the Helsinki University of Technology (HUT), Espoo, Finland, in 1995 and 1998, respectively, and is currently working towards the Dr.Sci. degree at HUT.

He is currently a Research Engineer in the Radio Laboratory, HUT. His current research interests are numerical dispersion and perfectly matched layers in FDTD method, the high-order finite-element method (FEM) applied to electromagnetic problems and the method of moments (MoM).

Mr. Juntunen has been awarded a position in a national graduate school GETA for 1996-2000. For the academic year 1998-1999 he was granted a European Union's Marie Curie Fellowship to work at the Aristotle University of Thessaloniki.

Theodoros D. Tsiboukis (S'79–M'81) was born in Larissa, Greece, on February 25, 1948. He received the Diploma degree in electrical and mechanical engineering from the National Technical University of Athens, Athens, Greece, in 1971, and the Dr. Eng. degree frm the Aristotle University of Thessaloniki, Thessaloniki, Greece, in 1981.

During the academic year 1981–1982, he was a Visiting Research Fellow in the electrical Engineering Department, University of Southampton, U.K. Since 1982, he has been with the Department of Electrical and Computer Engineering, Aristotle University of Thessaloniki, where he is currently a Professor. From 1993 to 1997, he was the Director of the Division of Telecommunications, Department of Electrical and Computer Engineering, Aristotle University of Thessaloniki, and in 1997, was elected the Chairman of this department from 1997 to 1999. He has authored six books, and has authored or co-authored over 60 refereed journal articles and over 50 conference papers. His research interests include electromagnetic-filed analysis by energy methods, computational electromagnetics [FEM, boundary-element method (BEM), vector finite elements, MoM, FDTD, and absorbing boundary conditions (ABC's)], and adaptive meshing in FEM analysis. He was the guest editor of a special issue on the *International Journal of Theoretical Electrotechniques* (1996) and the chairman of the local organizing committee of the 8th International Symposium on Theoretical Electrical Engineering (1995). He is a member of various societies, associations, chambers, and institutions. He has also organized and chaired conference sessions.

Dr. Tsiboukis has been awarded a number of distinctions.